Time-Resolved CIDNP Study of Non-Native States of Bovine and Human α-Lactalbumins

Olga B. Morozova,[†] P. J. Hore,[‡] Valentina E. Bychkova,[§] Renad Z. Sagdeev,[†,||] and Alexandra V. Yurkovskaya*[,†]

International Tomography Center of SB RAS, 630090, Institutskaya 3a, Novosibirsk, Russia, Department of Chemistry, University of Oxford, Physical and Theoretical Chemistry Laboratory, South Parks Road, Oxford, OX1 3QZ, United Kingdom, Institute of Protein Research RAS, Institutskaya 4, Puschino, Moscow region, Russia, and Center of Magnetic Tomography and Spectroscopy, Moscow State University, 119992, Leninskie Gory 1-73, Moscow, Russia

Received: October 11, 2004; In Final Form: January 14, 2005

The reaction mechanism and details of the formation of CIDNP (chemically induced dynamic nuclear polarization) in the photoreactions of the aromatic dye 2,2′-dipyridyl with non-native states of bovine and human α-lactalbumins (BLA and HLA) in aqueous solution have been studied using the time-resolved CIDNP technique. Non-native states have been obtained at pH 2 in the presence of 0, 8, and 10 M urea-d_4 and at pH 6.7 in the presence of 10 M urea-d_4. The dependence of the geminate CIDNP spectra of the two proteins on the denaturant concentration is shown to be determined by the intrinsic reactivity of the amino acid residues toward the triplet excited dye rather than by structural changes in the proteins. Values of the proton paramagnetic relaxation times (T_1) have been obtained from an analysis of the CIDNP kinetics. For tryptophan and tyrosine residues, the T_1 values change in opposite directions when the proteins are progressively denatured, reflecting the different internal mobilities of the two types of residues. It has been found that for both BLA and HLA the CIDNP kinetics of the non-native states formed at pH 6.7 in the presence of 10 M urea are almost identical to those at pH 2 with no urea, suggesting that the polarizable amino acid side chains have closely similar solvent accessibilities and motional properties in the two non-native states.

Introduction

Chemically induced dynamic nuclear polarization (CIDNP) is a high-sensitivity NMR technique for studying free radical reactions which has proved useful for elucidating organic reaction mechanisms and the structures of reactive intermediates. The observed nuclear polarization is determined by the magnetic resonance parameters of the transient radicals (*g*-factors and hyperfine coupling constants) and by the spin multiplicity of the radical pair precursor (see two monographs[1,2] and two major reviews[3,4]). An application of the CIDNP phenomenon has been devised to study the structures of biological macromolecules in which the intensities of certain lines in the NMR spectra of e.g. proteins are specifically enhanced.[4−6] The essence of this photo-CIDNP experiment is as follows. A protein solution containing a photosensitizer is irradiated in the NMR probe using a laser. Excited photosensitizer molecules react reversibly with aromatic amino acid side chains on the surface of the protein to generate dye−protein radical pairs in which spin-selective singlet−triplet transitions lead to nuclear polarization.[7] The back reaction of the radical pair yields nuclear spin polarization in the side chains of the reactive amino acid residues.[3,5] Of the 20 common amino acids only three (histidine, tyrosine, and tryptophan) are CIDNP-active.[5] The method has been used to study the surface structures of proteins and protein−ligand interactions and has recently been employed to follow protein folding reactions in real time, with ∼100 ms time-resolution, at the level of individual amino acid residues.[8−10] Compared to the lifetime of the free radicals in solution, this time scale corresponds to steady-state conditions for CIDNP formation and allows only semiquantitative interpretation of the CIDNP spectra. A time-resolved (TR) CIDNP method, however, which combines nanosecond pulsed laser excitation with NMR detection of nuclear polarization on a microsecond time scale,[11] offers the possibility of separating the contributions to the polarization from geminate radical pair recombination and from free radical reactions in the bulk and of performing a quantitative kinetic analysis of the nuclear polarization. In an ongoing project, we have applied TR-CIDNP to study amino acids,[12−14] small peptides,[15,16] and proteins.[17,18] This technique not only is applicable to studies of the structures of proteins and the changes in structure brought about by folding[19,20] but also provides the possibility of (a) detecting intramolecular electron transfer in proteins,[17] (b) measuring paramagnetic relaxation rates of protons in the radical forms of the solvent-exposed residues,[18] and (c) extracting information about intramolecular mobility of the polarizable side chains from the relaxation data.[18]

Partially unfolded and denatured states of proteins are functionally important in living cells,[21] as they are involved in translocation across membranes,[21] play a crucial role in the transition to amyloid fibrils,[22] and have anticancer activity by inducing apoptosis of tumor cells.[23] Non-native states usually possess conformational heterogeneity and complex dynamic properties.[24] They are generally quite difficult to study using conventional NMR spectroscopy, because the spectra often have broad lines due to the conformational fluctuations.

* To whom correspondence should be addressed. Tel: +7(3832)331333. Fax: +7(3832)331399. E-mail: yurk@tomo.nsc.ru.
[†] International Tomography Center of SB RAS.
[‡] Department of Chemistry, University of Oxford.
[§] Institute of Protein Research RAS.
[||] Center of Magnetic Tomography and Spectroscopy, Moscow State University.

10.1021/jp045367v CCC: $30.25
Published on Web 03/08/2005

Molten globules are partially folded states of proteins that frequently occur as intermediates in protein folding and have attracted much attention over the past 20 years.[25,26] The molten globule state characterized in most detail is that formed by α-lactalbumin.[25] In the native state, this small Ca^{2+}-binding protein (14 200 Da) performs an important function in mammary secretor cells as one of two components of lactose synthase, which catalyzes the final step in lactose biosynthesis in the lactating mammary glands (for a review of the structure and function of α-lactalbumins see ref 27). α-Lactalbumin can be partially unfolded to a molten globule state under a variety of mildly denaturing conditions.[25] Remarkable progress in analyzing the unfolding of a molten globule state has recently been achieved using two-dimensional (2D) $^{15}N-^{1}H$ heteronuclear single quantum coherence (HSQC) NMR applied to ^{15}N-labeled proteins.[28,29] It has been shown that in contrast to other globular proteins, unfolding of the molten globule state of α-lactalbumin is noncooperative.[28] A comparative study of the stability of bovine and human α-lactalbumins revealed that the human protein is considerably more resistant to urea-induced unfolding.[28]

In the present paper, we report a TR-CIDNP study of the urea-induced unfolding of the molten globule states of human and bovine α-lactalbumins (HLA and BLA, respectively). The two proteins have 76% amino acid sequence identity and possess closely similar structures in their native states.[30,31] The differences in sequence have a major influence on the stability of the two proteins toward unfolding by urea.[18] The aim is to explore the solvent-exposure and the dynamic properties of tryptophan and tyrosine residues under conditions of denaturant-induced unfolding and to test the ability of the TR-CIDNP technique to provide a quantitative description of the heterogeneity of the intramolecular dynamics of different residues in non-native states of HLA and BLA.

Experimental Section

A detailed description of the TR-CIDNP setup has been given previously.[18] The samples, sealed in a standard 5 mm NMR Pyrex ampule, were irradiated by a COMPEX Lambda Physik excimer laser (wavelength of 308 nm, pulse energy up to 150 mJ) in the probe of a 200 MHz Bruker DPX-200 NMR spectrometer. Light was guided to the sample using an optical system containing a quartz lens, a prism, and a cylindrical light-guide (5 mm diameter). TR-CIDNP experiments were carried out with the following pulse sequence: radio frequency (rf) saturation pulses; laser pulse; evolution time, τ; rf detection pulse; free induction decay. As the background signals in the spectrum originating from Boltzmann polarization are suppressed, only resonances from the polarized products formed during the variable delay τ appear in the CIDNP spectra. In all kinetic measurements, a rf pulse with duration of 4 μs was used. The timing corresponds to the center of the rf pulse (i.e., 2 μs for $\tau = 0$) on all plots in Figure 3.

Bovine α-lactalbumin, 2,2′-dipyridyl (DP), *N*-acetyl tryptophan, *N*-acetyl tyrosine, flavin mononucleotide (FMN), urea-d_4, and D_2O were used as received from Sigma-Aldrich. Human α-lactalbumin was obtained according to the procedure given in ref 32.

The concentrations were 1.3 mM for *N*-acetyl tryptophan, 1.3 mM for *N*-acetyl tyrosine, 1.5 mM for the proteins, and 2.5 mM for FMN. Due to the more than 10-fold difference in the absorption coefficients of protonated and neutral forms of 2,2′-dipyridyl ($pK_a = 4.3$), the concentrations used for DP were 14 mM at pH 6.7 and 0.6 mM at pH 2. The pH of the NMR samples was adjusted by addition of DCl. No correction was made for the deuterium isotope effect on the pH.

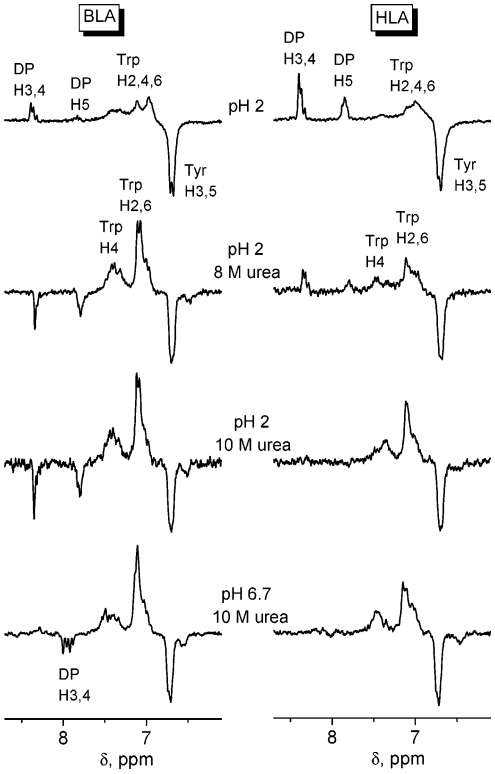

Figure 1. Aromatic region of ^{1}H CIDNP spectra, obtained for bovine (left) and human (right) α-lactalbumins with 2,2′-dipyridyl under various experimental conditions. The spectra were taken immediately after the laser pulse.

Results

Bovine α-lactalbumin contains 11 potentially polarizable residues: 4 tyrosines (Tyr16, Tyr36, Tyr50, and Tyr103), 3 histidines (His32, His68, and His 107), and 4 tryptophans (Trp26, Trp60, Trp108, and Trp118). In human α-lactalbumin, the residues His68 and Trp26 are replaced by Gln68 and Leu26, respectively. Figure 1 shows CIDNP spectra obtained for non-native states of BLA and HLA polarized by DP under a variety experimental conditions: at pH 2 in the presence of 0, 8, and 10 M urea-d_4 and at pH 6.7 in the presence of 10 M urea-d_4. All spectra were recorded immediately after the laser pulse ($\tau = 0$). The vertical scales of the eight spectra were separately adjusted to get approximately equal intensities for the emissive aromatic tyrosine resonance.

The spectra in Figure 1 exhibit the following features: (1) Histidine residues (including His68 of BLA which has the highest CIDNP intensity in the native state[18]) do not appear in the CIDNP spectra of the non-native states. (2) The intensity of the Trp signal relative to the Tyr signal is always larger for BLA than for HLA under the same conditions. The emissive contribution to the enhancement of the DP resonances is also larger for BLA. (3) For both proteins, the Trp signals become stronger relative to those of the Tyr residues on addition of urea at pH 2. The emissive contribution to the polarization of the DP resonances also increases when urea is added. (4) For both proteins at neutral pH in the presence of 10 M urea, the relative intensities of the polarized signals are very similar to those observed at pH 2, also with 10 M urea.

Measurements have also been made for denatured states of BLA using FMN as the photosensitizer. Flavins, including FMN,

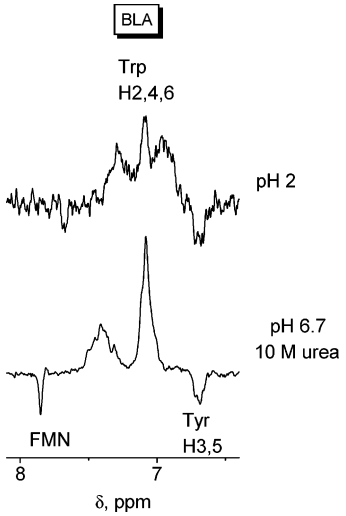

Figure 2. Aromatic region of ^{1}H CIDNP spectra, obtained for bovine α-lactalbumin with flavin mononucleotide at pH 2 (upper) and at pH 6.7 with 10 M urea-d_4 (lower). The spectra were taken immediately after the laser pulse.

have been extensively used to generate CIDNP in proteins in earlier studies.[3,8,20,33] CIDNP spectra of BLA obtained with FMN at pH 2 and pH 6.7, measured immediately after the laser pulse, are shown in Figure 2. At pH 2, the signal-to-noise ratio is much lower than is obtained with DP (Figure 1). The kinetic data obtained using FMN at pH 2 were too noisy to allow satisfactory quantitative analysis: measurements of the time-resolved CIDNP intensities were therefore restricted to those photosensitized by DP.

CIDNP kinetics for both proteins obtained under different experimental conditions are shown in Figure 3. The spectra were integrated over the chemical shift ranges 6.85−7.67 and 6.46−6.83 to get the signal intensities of the Trp and Tyr residues, respectively. All sets of measurements have been scaled to unity at the first point ($\tau = 0$). The following features can be seen: (1) For the Trp signals, the stationary value of the CIDNP intensity (at $\tau = 1$ ms) relative to the initial value (at $\tau = 0$) increases as the urea concentration is increased at pH 2. The opposite is found for the Tyr residues. (2) Under the same conditions, the stationary value ($\tau = 1$ ms) of the CIDNP intensity of HLA relative to the initial value is equal to or higher than that for BLA, for both Trp and Tyr residues. (3) Closely similar CIDNP kinetics were found at pH 2 without urea and at pH 6.7 with 10 M urea, for both types of polarized residue in both BLA and HLA.

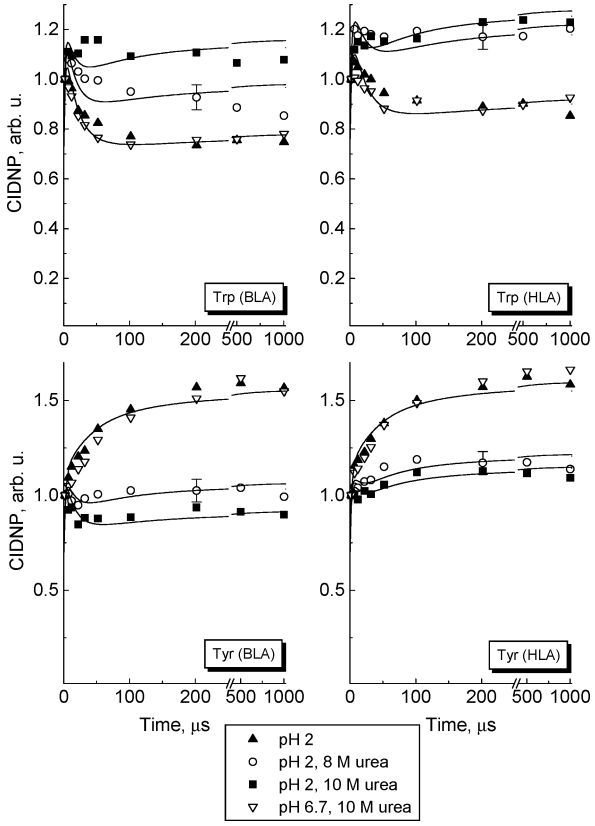

Figure 3. ^{1}H CIDNP kinetics, obtained for tryptophan (upper) and tyrosine (lower) residues of bovine (left) and human (right) α-lactalbumins with 2,2′-dipyridyl under various experimental conditions: pH 2, no urea (▲); pH 2, 8 M urea (○); pH 2, 10 M urea (■); pH 6.7, 10 M urea (▽). The solid lines are the best fit simulations calculated according to the procedure described in the text. For the parameter values, see Table 1.

Discussion

CIDNP Spectra. The CIDNP signal intensity observed for an amino acid residue in a protein depends on the reactivity of its side chain toward the photoexcited dye.[34] The reactivity is considered as the quenching rate constant for a completely accessible side chain scaled by a factor that characterizes the accessibility of the residue. We have previously reported the pH-dependence of the rate constants, k_q, of the reactions between triplet DP and the *N*-acetyl derivatives of tryptophan,[12] tyrosine,[13] and histidine.[14] The lowest reactivity was observed for histidine. No reaction takes place under acidic conditions between the triplet DP cation (^{T}DPH$^+$, p$K_a = 5.8$) and histidine carrying a positive charge on the imidazole ring (HisH$^+$, p$K_a = 6.1$). However a reaction does occur between the neutral triplet, ^{T}DP, and HisH$^+$. The pH dependence of k_q for *N*-acetyl histidine is characterized by a maximum value of 4×10^7 M^{-1} s^{-1} at pH 6,[14] which is more than an order of magnitude smaller than that for tryptophan[12] and tyrosine,[13] such that if an equimolar mixture of the three amino acids is studied at neutral pH, no histidine signal is observed in the CIDNP spectrum as a result of competition effects.[18] For the native state of BLA, His68 is polarizable owing to the very high accessibility of its side chain compared to the other CIDNP-active residues.[30] The absence of histidine signals for the non-native state of BLA at pH 6.7 in the presence of 10 M urea (Figures 1 and 2) indicates an increased accessibility of the Trp and Tyr residues such that the His residues can no longer compete effectively for the triplet excited dye. At pH 2, His signals are not expected (see above), nor are they observed.

The phases of the aromatic proton polarizations of the amino acid residues (enhanced absorption for Trp and emission for Tyr) are in accordance with Kaptein's rules.[7] The DP polarization is formed in two types of radical pairs, with the partner radical originating from a Trp or a Tyr residue. The *g*-values of the radicals increase in the sequence g(Trp) < g(DP) < g(Tyr), resulting in emission for DP formed from a radical pair containing a Trp radical[12] and absorption for a pair containing a Tyr radical.[13] Thus, the sign and relative intensity of the DP signal reflects the relative numbers of Trp and Tyr radicals formed by the reactions of ^{T}DP.

On addition of urea, the increase in the relative intensity of the Trp signals together with the growth of the emissive contribution to the DP signal suggests an increasing fraction of radical pairs containing a Trp radical. This could arise either from a change in the intrinsic reactivity of tryptophan and

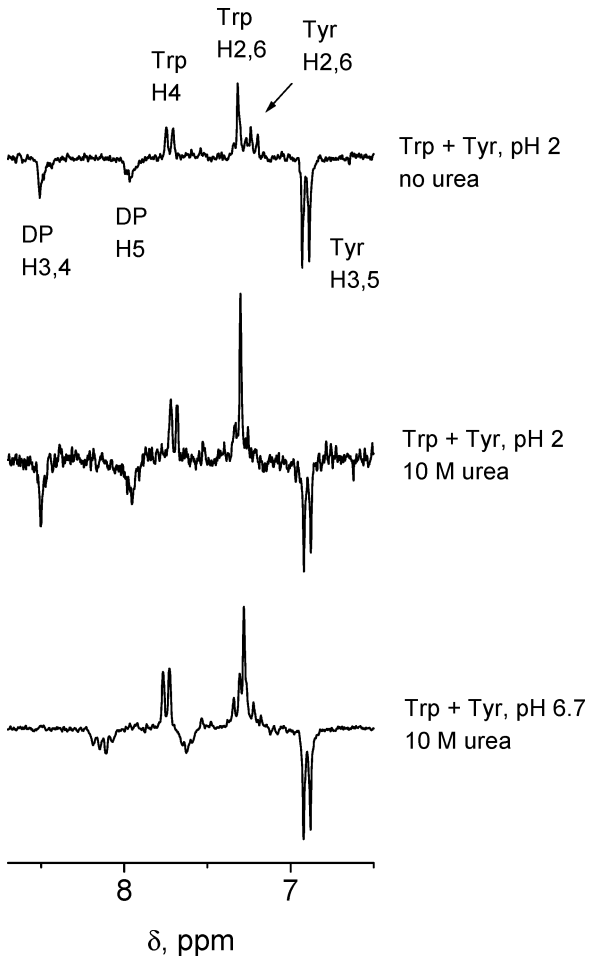

Figure 4. Aromatic region of ^{1}H CIDNP spectra, obtained for an equimolar mixture of *N*-acetyl tryptophan and *N*-acetyl tyrosine with 2,2′-dipyridyl under various experimental conditions. The spectra were taken immediately after the laser pulse.

tyrosine side chains in the presence of urea or because the urea-induced denaturation affects the accessibility of Trp and Tyr residues in different ways.

To clarify the origin of these changes, we have measured geminate CIDNP spectra of equimolar mixtures of tryptophan and tyrosine amino acids at pH 2 with and without 10 M urea and at pH 6.7 with 10 M urea. Figure 4 shows that the same trend is observed for the amino acids as for BLA and HLA (Figure 1). The Trp enhancement relative to that of Tyr is increased by approximately a factor of 2 by 10 M urea for both the mixture of amino acids and the two proteins. Thus, it is the intrinsic reactivity of the amino acids, rather than structural changes in the proteins, that is responsible for the dependence of the geminate spectra of BLA and HLA on the denaturant concentration.

In the native three-dimensional fold of α-lactalbumin (Figure 5) are two domains connected by the calcium binding loop and divided by a deep cleft.[25,27] The larger domain, the α-domain, is predominantly helical and includes four major helices A, B, C, and D comprising residues 5−11, 23−34, 86−99, and 105−109, respectively, and three short 3_{10} helices (residues 12−16, 101−104, and 115−119). All four tryptophan residues (26, 60, 104, and 118) are located in this α-domain. The *β*-domain is smaller and is composed of a series of small loops, a small triple-stranded antiparallel *β*-pleated sheet (residues 40−56), and a 3_{10} helix (residues 76−82). Of the four tyrosine residues, Tyr50 is in the *β*-domain in the *β*-sheet, Tyr18 and Tyr103 are in the α-domain, and Tyr36 is located in the loop between the

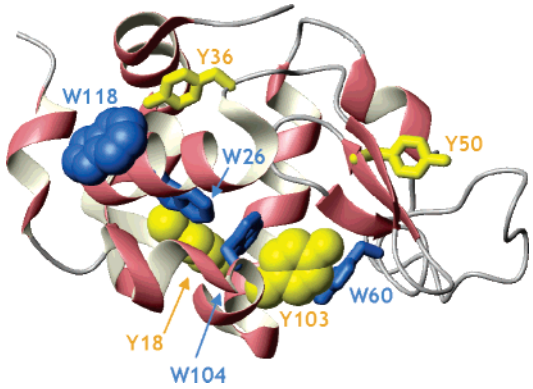

Figure 5. Ribbon representation of the three-dimensional structure of bovine α-lactalbumin. The side chains of the tryptophan (blue) and tyrosine (yellow) residues are shown. Side chains that are CIDNP-active in the native state are shown as space-filled. The diagram was generated using the PDB coordinates for BLA (1F6S) (ref 30) with the program MOLMOL 2K.1 (ref 37).

B-helix and the *β*-pleated sheet in the *β*-domain. Hydrogen exchange protection factors have been measured for molten globule states of different α-lactalbumins.[29,35,36] In both HLA and BLA, residues in the *β*-domain were found to be substantially less protected than those in the α-domain. Within the α-domain, the largest protection was found in the B-helix and the smallest in the A-helix. The method is not applicable to the D-helix, since it is not protected in the native state. The unfolding of the molten globule state was found to be highly noncooperative for both proteins. The urea-induced unfolding of individual residues was followed via 3D ^{15}N-edited nuclear Overhauser enhancement spectroscopy (NOESY)-HSQC spectra of the molten globule states of HLA and BLA.[28,29] Resolved resonances are only observed for residues that are in unfolded regions of the polypeptide chain. In the absence of urea, only two peaks are visible for BLA, and additional peaks appear progressively as the concentration of urea is increased. The main conclusion is that the α-domain is more resistant to unfolding than the *β*-domain. The urea concentrations (in mol dm^{-3}) at which the ^{1}H−^{15}N HSQC cross-peak of each CIDNP-active residue has 20−25% of the intensity observed for the same residue in the fully unfolded protein (BLA/HLA) are as follows:[29] 11.5/− (Trp26), 11/11 (Trp60), 8/12.5 (Trp104), 10.5/14.5 (Trp118), 5/9 (Tyr18), 1/3 (Tyr36), 4/4 (Tyr50), and 8/10 (Tyr103). These data indicate that the peaks of the tryptophan residues in the denatured states of both proteins appear at higher urea concentrations than those of the tyrosines. For the same residues, the corresponding values of urea concentration for BLA are generally lower than those for HLA.

The HSQC experiments identify a stable core region in the structure of the molten globule states, involving the A-, B-, and D-helices and the C-terminal 3_{10} helix, which remains compact even under extreme denaturing conditions.[28,29] Detailed characterization revealed that among the eight key residues identified as being involved in stabilizing the molten globule of HLA,[28] the only CIDNP-active residues are Trp118, which is present in both proteins, and Trp26 in BLA which is replaced by Leu in HLA. The fact that in all cases the relative intensity of the Trp signal is lower for HLA compared to BLA indicates that Trp26 might give a contribution to the polarization pattern in BLA. The detection of a polarized signal from Trp118 in the native states of both BLA and HLA, for which the calculated accessibilities are 13.5% and 10%, respectively, leads to the conclusion that even rather low solvent exposure may be sufficient for CIDNP formation.[18]

CIDNP Kinetics. The processes that govern the kinetics of the CIDNP formed in reversible radical reactions are nuclear paramagnetic relaxation and radical reactions, including termination and electron transfer. The latter can be degenerate electron exchange between residues of the same kind and/or intramolecular electron transfer (IET) between residues of different types. The CIDNP kinetics of denatured hen lysozyme, produced either by raising the temperature at pH 3.8 or by addition of 10 M urea, are influenced by IET from tyrosine residues to tryptophan radicals.[17] We have examined the possibility of IET reactions occurring under the conditions used in the present investigation by studying the CIDNP kinetics of the peptide tryptophan−tyrosine, a model system in which IET is highly efficient. It was found that at pH 2, with and without 10 M urea, the electron-transfer reaction is fast (rate constant $\sim 10^5$ s^{-1}) and reversible.[38] Since α-lactalbumin contains a pair of neighboring tyrosine/tryptophan residues, Tyr103 and Trp104, IET could be occurring here as well. As the low spectral resolution does not allow one to distinguish the contributions from individual residues, we made an attempt to take IET into account in the analysis of the overall CIDNP effects. The theoretical description of CIDNP kinetics in the presence of IET involves treating the kinetics of the dye and the tryptophan and tyrosine residues by a set of coupled differential equations with common values of IET rate constants.[16] It proved impossible to describe the present set of kinetics according to the procedure used for the peptide,[16,38] with a self-consistent set of parameters. In particular, satisfactory simulation of the CIDNP kinetics of the Trp and Tyr residues required different values of the IET rate constants. In addition, the characteristic time of the second-order radical termination for dipyridyl radical obtained for the best fit was unrealistically long (~100 μs). It thus seems that IET does not make a significant contribution to the overall CIDNP kinetics in denatured α-lactalbumins.

The observed CIDNP kinetics were interpreted using an approach due to Fischer et al.[39,40] in which the radical concentration $R(t)$ and the nuclear polarizations of the radicals $P(\mathrm{R})$ and the diamagnetic products $P(\mathrm{Pr})$ are described by the differential equations:

$$R(t) = \frac{R_0}{1 + k_t R_0 t} \tag{1}$$

$$\frac{\mathrm{d}P(\mathrm{R})}{\mathrm{d}t} = -k_t P(\mathrm{R}) R - k_t \beta R^2 - \frac{P(\mathrm{R})}{T_1} \tag{2}$$

$$\frac{\mathrm{d}P(\mathrm{Pr})}{\mathrm{d}t} = k_t P(\mathrm{R}) R + k_t \beta R^2 \tag{3}$$

where R_0 is the initial radical concentration, k_t is the radical termination rate constant, T_1 is the nuclear paramagnetic spin−lattice relaxation time in the radicals, and the parameter β represents the polarization per pair, created in F-pairs. In most cases, $\beta \approx 3P^G/R_0$,[40] where P^G is the geminate polarization at $t = 0$. The first terms on the right side of eqs 2 and 3 describe the transfer of polarization from the radicals to the diamagnetic molecules in the termination reaction; the second terms represent the formation of polarization in F-pairs. The third term in eq 2 corresponds to the loss of polarization in the radicals due to nuclear paramagnetic relaxation. It was assumed that the yield of radicals that escape from the triplet geminate radical pair is much greater than the yield of geminate recombination and that the radical pair partners disappear only by recombining with one another (with rate constant k_t). The initial polarizations were taken as $P(\mathrm{Pr}) = P^G = -P(\mathrm{R})$, which is consistent with the spin-sorting nature of the $S-T_0$ radical pair mechanism.

TABLE 1: Nuclear Paramagnetic Relaxation Times, Correlation Times, and Second-Order Termination Rate Constants Used in the Simulation of CIDNP Kinetics of BLA and HLA at pH 2 at Different Urea Concentrations

residue (protein), urea concn/M	$R_0k_t/10^5$ s^{-1}	T_1/μs	$\tau_c(pr)$/ns	τ_e/ns
Trp (BLA), 0	2.0	60	6.8	25.8
Trp (BLA), 8	2.0	38	4.3	5.0
Trp (BLA), 10	2.0	28	3.1	3.1
Trp (HLA), 0	1.5	60	6.8	30.8
Trp (HLA), 8	1.5	38	4.3	5.1
Trp (HLA), 10	1.5	28	3.1	3.1
Tyr (BLA), 0	1.3	16	0.8	0.9
Tyr (BLA), 8	1.9	28	0.25	0.25
Tyr (BLA), 10	2.0	37	0.18	0.18
Tyr (HLA), 0	1.3	16	0.8	0.9
Tyr (HLA), 8	1.9	21	0.35	0.35
Tyr (HLA), 10	2.0	21	0.35	0.35

Strictly speaking, the disappearance of the radicals is not characterized by a single termination rate constant k_t. If more than one amino acid residue can be polarized, the reactions of the dye radicals with the radicals derived from the exposed aromatic side chains should be treated as parallel processes. This would require knowledge of many parameters, e.g., the initial radical concentrations and the second-order termination rate constants for each of the reactive residues, which cannot be determined from the available experimental data. We have therefore used a simplified approach, treating the reactions of the dye with each of the polarizable aromatic residues as independent chemical processes. The parameters introduced above affect the shape of the CIDNP kinetics in the following way: a decrease in T_1 and/or an increase in k_t leads to a larger stationary CIDNP intensity with respect to the initial intensity.

Increasing the urea concentration affects the Tyr- and Trp-residue CIDNP kinetics in different ways: for tyrosine, a decrease in the stationary CIDNP signal with respect to the geminate polarization was detected, while for tryptophan, the stationary CIDNP increased. Bearing in mind that progressive unfolding on addition of denaturant is likely to affect the intramolecular mobility of the polarizable residues, we suggest that a plausible way to explain the observed CIDNP kinetics is to consider the variation of their nuclear paramagnetic relaxation times T_1. We have analyzed the kinetic measurements accordingly and summarize the results in Table 1, in which T_1 and R_0k_t are the parameters of the best fit simulations shown in Figure 3. The main features of these results are the following. (a) The CIDNP kinetics of Trp in BLA are characterized by a relatively large value of R_0k_t. (b) The values of T_1 for the Trp protons were the same for BLA and HLA. (c) The product of initial radical concentration and the second order termination rate constant is independent of the urea concentration for the Trp kinetics. (d) To describe the changes in the kinetics of Tyr, both R_0k_t and T_1 had to be varied. (e) The Tyr kinetics in BLA and HLA were characterized by the same R_0k_t, but different T_1 values.

Mobility of Amino Acid Residues. The paramagnetic relaxation times T_1 may be assumed to depend on the motional correlation time τ_c according to the relation[41]

$$\frac{1}{T_1} = \frac{(\Delta B)^2 \tau_c}{1 + (\omega_N \tau_c)^2} \tag{4}$$

where ΔB is the strength of the local magnetic field whose stochastic modulation is responsible for the relaxation, and ω_N is the nuclear Larmor frequency.

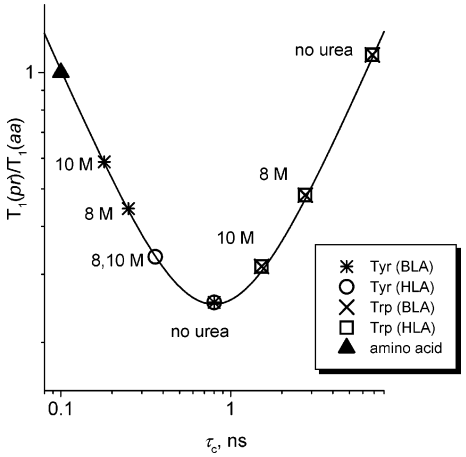

Figure 6. Calculated dependence of the ratio of the nuclear paramagnetic relaxation times for the protein and the free amino acid T_1(pr)/T_1(aa) on the rotational correlation time τ_c(pr) according to eq 6 for a nuclear Larmor frequency $\omega_N = 2\pi \times 200$ MHz. The symbols show the values of T_1(pr)/T_1(aa) extracted from the simulations of the CIDNP kinetics. The urea concentrations are as indicated.

For the free amino acids, assuming that the rotational correlation time of the corresponding radical τ_c(aa) is likely to be approximately 100 ps, we have $(\omega_N\tau_c)^2 \ll 1$ for an NMR frequency $\omega_N = 2\pi \times 200$ MHz. Therefore,

$$\frac{1}{T_1(\text{aa})} = (\Delta B)^2 \tau_c(\text{aa}) \tag{5}$$

In our previous studies, we have determined the following values for the nuclear paramagnetic relaxation times, T_1(aa), in the amino acid radicals by fitting the experimental CIDNP kinetics: 63 μs for Tyr H3,5,[13] 44 μs for Trp H2,6, and 63 μs for Trp H4.[12]

If we assume that ΔB is the same for the free amino acid and the corresponding residue in a protein, we can obtain the following expression, where T_1(pr) and τ_c(pr) are the measured nuclear paramagnetic relaxation time and the effective correlation time for the side chain radical in the protein:

$$\frac{T_1(\text{pr})}{T_1(\text{aa})} = \frac{\tau_c(\text{aa})}{\tau_c(\text{pr})}[1 + [\omega_N\tau_c(\text{pr})]^2] \tag{6}$$

$\tau_c(\text{pr})^{-1} = \tau_M^{-1} + \tau_e^{-1}$, with τ_M referring to the rotation of the whole protein and τ_e corresponding to the intramolecular motion of the residue in the molecular reference frame. Figure 6 shows the calculated dependence of T_1(pr)/T_1(aa) on τ_c(pr) for $\omega_N = 2\pi \times 200$ MHz. Experimental values of T_1(pr)/T_1(aa) were calculated using T_1(pr) obtained from the CIDNP kinetics (see Table 1) and the T_1(aa) values above.[12,13] T_1(aa) of the Trp H2,4,6 protons was taken as 54 μs, the mean of 44 and 63 μs.[12]

Each experimental value of T_1(pr)/T_1(aa) corresponds to two values of τ_c(pr), except at the minimum of the function. It is reasonable to assume that urea-induced disruption of the native structure of the protein leads to a decrease in the correlation time for the internal motion of the residues. Therefore, for each value of T_1(pr)/T_1(aa), we have chosen the τ_c(pr) value that ensures that τ_c(pr) decreases as the urea concentration is increased. The resulting values of τ_c(pr) are listed in Table 1.

Values of the correlation time for the rotation of a protein molecule as a whole can be calculated from its hydrodynamic radius R_S using Stokes' law, $\tau_M = 4\pi\eta R_S^3/3k_BT$, in which η is the viscosity of the solution, k_B is Boltzmann's constant, and T is the temperature. Values of R_S for BLA and HLA at pH 2 and different urea concentrations were measured using the NMR diffusion technique.[28] Viscosity data for aqueous solutions of urea were taken from ref 42. The calculated τ_M values (in nanoseconds) for BLA/HLA at pH 2 are 9.2/8.7 (no urea), 30.6/27.3 (8 M urea), and 43.3/38.9 (10 M urea). In this way, we calculated the correlation times for internal motion, τ_e, listed in Table 1.

Figure 6 may be understood by noting that the tryptophan residues in α-lactalbumin are located in the parts of the polypeptide chain that are relatively resistant to denaturation (see above) and which might, therefore, have a lower degree of internal mobility. Although the motional correlation times of all the polarizable residues decrease when the protein unfolds, the T_1 values of Tyr and Trp residues appear to fall on either side of the minimum in the variation of T_1(pr) with τ_c(pr). This may explain the opposing trends for the CIDNP kinetics of Trp and Tyr resonances upon increasing the denaturant concentration.

It is interesting to note that the A-states of both proteins (at pH 2) and the denatured states at neutral pH with 10 M urea have identical CIDNP kinetics. Although the CIDNP spectra detected under these conditions look somewhat different, close inspection shows that the protein signals have common features. First, the relative enhancements of the Trp and Tyr resonances for these two states agree well with the relative reactivities of the residues under these conditions, obtained from a comparison with the CIDNP spectra of mixtures of the amino acids. Second, although the chemical shifts differ, the line widths of the polarized protein resonances are comparable. More significantly, however, extremely similar kinetics are observed for the two types of residue (Trp or Tyr) in the two states of both proteins, using both FMN (not shown) and DP (Figure 3, open and filled triangles) as photosensitizer. Since the correlation time for the tryptophan residues is determined mainly by the rotation of the protein as a whole ($\tau_c(\text{pr}) \approx \tau_M$), while internal motions are responsible for the correlation time for the tyrosine residues ($\tau_c(\text{pr}) \approx \tau_e$), we conclude that the side chains of the polarizable aromatic residues in the two states of both α-lactalbumins have similar dynamics.

Conclusion

A comparative study of the pH 2 molten globule state and the urea-denatured states of bovine and human α-lactalbumins is presented as a continuation of our systematic study of proteins and protein-related compounds using the time-resolved CIDNP technique. We have shown that the relative intensities of the signals in the geminate CIDNP spectra can be used to shed light on the accessibility and reactivity of amino acid residues toward the excited dye molecules in a manner similar to that employed for the native state.

The spectral resolution for the partially folded states studied here is relatively low due to slow conformational exchange. An inevitable consequence is the impossibility of analyzing, separately, the kinetics of the CIDNP effects for individual residues. As a result, certain details of the radical reactions responsible for the nuclear polarization could not be extracted, in particular the contribution of intramolecular electron transfer involving the neighboring residues, Tyr103 and Trp104. Analysis of the CIDNP kinetics allows the determination of the nuclear spin−lattice relaxation times of radicals derived from the reactive tyrosine and tryptophan residues, opening the possibility of obtaining qualitative information about the correlation times of their intramolecular motion. Values of T_1 for the paramagnetic states of the tryptophan and tyrosine residues were found to

have opposite dependence on the motional correlation time reflecting the different degrees of crowding and motional restriction imposed by neighboring side chains.

Acknowledgment. The financial support of INTAS (Project No. 02-2126), RFBR (Projects 02-03-32765 and 05-03-32370), and the Royal Society (International Joint Project Grant Programme) is gratefully acknowledged. A.V.Y. and O.B.M. are indebted to the Russian Science Support Foundation for financial support. We are grateful to Dr. Ken Hun Mok for helpful discussions and preparing Figure 5.

References and Notes

(1) *Chemically Induced Magnetic Polarization*; Muus, L. T., Atkins, P. W., McLauchlan, K. A., Pedersen, J. B., Eds.; D. Reidel: Dordrecht, 1977.

(2) Salikhov, K. M.; Molin, Y. N.; Sagdeev, R. Z.; Buchachenko, A. L. *Spin Polarization and Magnetic Field Effects in Radical Reactions*; Molin Yu. N., Ed.; Elsevier: Amsterdam, 1984.

(3) Hore, P. J.; Broadhurst, R. W. *Prog. NMR Spectrosc.* **1993**, *25*, 345−402.

(4) Kaptein, R. *Biol. Magn. Reson.* **1982**, *4*, 145−149.

(5) Kaptein, R.; Dijkstra, K.; Nicolay, K. *Nature* **1978**, *274*, 293−294.

(6) Kaptein, R. Structural information from photo-CIDNP in proteins. In *NMR Spectroscopy in Molecular Biology*; Pullman, B., Ed.; D. Reidel: Dordrecht, 1978; pp 211−229.

(7) Kaptein, R. *J. Chem. Soc., Chem. Commun.* **1971**, 732.

(8) Lyon, C. E.; Suh, E.-S.; Dobson, C. M.; Hore, P. J. *J. Am. Chem. Soc.* **2002**, *124*, 13018−13024.

(9) Dobson, C. M.; Hore, P. J. *Nat. Struct. Biol., NMR Suppl.* **1998**, *5*, 504−507.

(10) Wirmer, J.; Kühn, T.; Schwalbe, H. *Angew. Chem.* **2001**, *113*, 4378−4380.

(11) Closs, G. L.; Miller, R. J. *J. Am. Chem. Soc.* **1979**, *101*, 1639−1644.

(12) Tsentalovich, Y. P.; Morozova, O. B.; Yurkovskaya, A. V.; Hore, P. J. *J. Phys. Chem. A* **1999**, *103*, 5362−5368.

(13) Tsentalovich, Y. P.; Morozova, O. B. *J. Photochem. Photobiol., A* **2000**, *30*, 33−40.

(14) Tsentalovich, Y. P.; Morozova, O. B.; Yurkovskaya, A. V.; Hore, P. J.; Sagdeev, R. Z. *J. Phys. Chem. A* **2000**, *104*, 6912−6916.

(15) Morozova, O. B.; Yurkovskaya, A. V.; Tsentalovich, Y. P.; Forbes, M. D. E.; Sagdeev, R. Z. *J. Phys. Chem. B* **2002**, *106*, 1455−1460.

(16) Morozova, O. B.; Yurkovskaya, A. V.; Vieth, H.-M.; Sagdeev, R. Z. *J. Phys. Chem. B* **2003**, *107*, 1088−1096.

(17) Morozova, O. B.; Yurkovskaya, A. V.; Tsentalovich, Y. P.; Forbes, M. D. E.; Hore, P. J.; Sagdeev, R. Z. *Mol. Phys.* **2002**, *100*, 1187−1195.

(18) Morozova, O. B.; Yurkovskaya, A. V.; Sagdeev, R. Z.; Mok, H. K.; Hore, P. J. *J. Phys. Chem. B* **2004**, *108*, 15355−15363.

(19) Lyon, C. E. Photo-CIDNP and Protein Folding. D. Phyl. Thesis, Oxford University, Oxford, U.K., 1999.

(20) Hore, P. J.; Winder, S. L.; Roberts, C. H.; Dobson, C. M. *J. Am. Chem. Soc.* **1997**, *119*, 5049−5050.

(21) Bychkova, V. E.; Pain, R. H.; Ptitsyn, O. B. *FEBS Lett.* **1988**, *238*, 231−234.

(22) Kelly, J. W. *Curr. Opin. Struct. Biol.* **1998**, *8*, 101−106.

(23) Svenson, M.; Sabharwal, H.; Hakansson, A.; Mossberg, A. K.; Lipniunas, P.; Leffler, H.; Svanborg, C.; Linse, S. *J. Biol. Chem* **1999**, *274*, 6388−6396.

(24) *Mechnisms of protein folding*; Pain, R. H., Ed.; Oxford University Press: New York, 2000.

(25) Kuwajima, K. *FASEB J.* **1996**, *10*, 102−109.

(26) Kühn, T.; Schwalbe, H. *J. Am. Chem. Soc.* **2000**, *122*, 6169−6174.

(27) Permyakov, E. A.; Berliner, L. J. *FEBS Lett.* **2000**, *473*, 267−274.

(28) Wijesinha-Bettoni, R.; Dobson, C. M.; Redfield, C. *J. Mol. Biol.* **2001**, *312*, 261−273.

(29) Schulman, B. A.; Kim, P. S.; Dobson, C. M.; Redfield, C. *Nat. Struct. Biol., NMR Suppl.* **1997**, *4*, 630−634.

(30) Chrysina, E. D.; Brew, K.; Acharya, K. R. *J. Biol. Chem.* **2000**, *275*, 37021−37029.

(31) Ren, J.; Stuart, D. I.; Acharya, K. R. *J. Biol. Chem.* **1993**, *268*, 19292−19298.

(32) Philips, N. I.; Jennes, R. *Biochim. Biophys. Acta* **1971**, *229*, 407−410.

(33) Lyon, C. E.; Lopez, J. J.; Cho, B.-M.; Hore, P. J. *Mol. Phys.* **2002**, *100*, 1261−1269.

(34) Winder, S. L.; Broadhurst, R. W.; Hore, P. J. *Spectrochim. Acta A* **1995**, *51*, 1753−1761.

(35) Schulman, B. A.; Redfield, C.; Peng, Z.-y.; Dobson, C. M.; Kim, P. S. *J. Mol. Biol.* **1995**, *253*, 651−657.

(36) Forge, V.; Wijesinha, R. T.; Balbah, J.; Brew, K.; Robinson, C. V.; Redfield, C.; Dobson, C. M. *J. Mol. Biol.* **1999**, *288*, 673−688.

(37) Koradi, R.; Billeter, M.; Wüthrich, K. *J. Mol. Graphics* **1996**, *14*, 51−55.

(38) Morozova, O. B.; Yurkovskaya, A. V.; Sagdeev, R. Z. *J. Phys. Chem. B* **2005**, *109*, 3668−3675.

(39) Vollenweider, J.-K.; Fischer, H.; Hennig, J.; Leuschner, R. *Chem. Phys. Lett.* **1985**, *97*, 217−234.

(40) Vollenweider, J.-K.; Fischer, H. *Chem. Phys.* **1988**, *124*, 333−345.

(41) Cavanagh, J.; Fairbrother, W. J.; Palmer, A. G.; Skelton, N. J. *Protein NMR spectroscopy*: *Principles and practice*; Elsevier: San Diego, 1996.

(42) *Handbook of Chemistry and Physics*, 83rd ed.; Lide, D. R., Ed.; CRC Press: Boca Raton, FL, 2003.